Document Number
TRACOR 66-342-U
Contract Number NObsr-91229
Project Serial No. SF101-03-17
Task 8139

CLEARINGHOUSE
FOR FEDERAL SCIENTIFIC AND
TECHNICAL INFORMATION

Hardcopy	Microfiche		
$ 2.00	$ .50	42 pp	

ARCHIVE COPY

code 1

AD 683973

A SUMMARY REPORT

ANALYTICAL STUDIES OF DOME-TRANSDUCER INTERACTIONS

Submitted to

Commander, Naval Ship Systems Command
Department of the Navy
Washington, D. C. 20360
Attention: Code 1622E

June 9, 1966

TRACOR INC.
6500 TRACOR LANE • AUSTIN, TEXAS 78721 • 512 926-2800

TRACOR, INC. 6500 TRACOR LANE, AUSTIN, TEXAS 78721

Document Number
TRACOR 66-342-U
Contract Number NObsr-91229
Project Serial No. SF101-03-17
Task 8139

A SUMMARY REPORT

ANALYTICAL STUDIES OF DOME-TRANSDUCER INTERACTIONS

Submitted to

Commander, Naval Ship Systems Command
Department of the Navy
Washington, D. C. 20360
Attention: Code 1622E

June 9, 1966

Approved by:
A. F. Wittenborn
A. F. Wittenborn
Technical Director

Prepared by:
W. C. Moyer
W. C. Moyer
Project Director

ABSTRACT

This report summarizes analytical studies conducted during the past year to determine the interaction of sonar domes and transducers during transmission. A general description of the mathematical model used in the analysis is given together with some improvements which have been incorporated in the model during the past year. The results of a study of the dependence of certain performance criteria such as directivity index on the parameters of the dome-transducer model is reviewed. In addition, a general description of developments related to the treatment of viscoelastic dome materials and nonconcentric dome shapes is given.

The conclusions drawn in the various technical memoranda submitted during the year are restated in this report. Briefly these are: (a) the dome tends to offset the gains in side lobe reduction obtained by shading the transducer elements, and (b) the most important property of the dome model in determining its effects on various transducer performance criteria is its surface density (product of mass density and thickness). These conclusions are supported by numerical results presented in the report. Finally, some recommendations for the continuance of studies of dome-transducer interactions are given. These include an emphasis on the development of a dome-transducer model of more general configuration and the desirability of an experimental program to support the analytical studies.

TABLE OF CONTENTS

	Page
Abstract	ii
List of Figures	iv
I. Introduction	1
II. Background	3
III. Discussion of Analytical Developments	8
IV. Conclusions	22
V. Recommendations	24
VI. References	25
VII. Acknowledgements	26
Appendix	27

LIST OF FIGURES

Figure No. Text		Page
1	Geometry for a Cylindrical Transducer Radiating in a Concentric Dome	5
2	Sound Pressure Distribution (dB) for a Transducer Radiating Inside a Concentric Dome (Nearfield)	10
3	Sound Pressure Distribution (dB) for a Transducer Radiating Inside a Concentric Dome (Farfield)	11
4	Comparison of Sound Pressure Distributions (dB) for a Transducer Radiating With and Without a Concentric Dome — Cosine Shading	12
5	Comparison of Sound Pressure Distributions (dB) for a Transducer Radiating With and Without a Concentric Dome — Tchebycheff Shading	13
6	Directivity Index VS Dome Surface Density $\rho_s h$	15
7	Side Lobe Level VS Dome Surface Density $\rho_s h$	16
8	Major Lobe Width VS Dome Surface Density $\rho_s h$	17

Figure No. Text		Page
9	Transmission Coefficient VS Dome Surface Density $\rho_s h$	18
10	Transfer Coefficient VS Dome-Transducer Spacing $\frac{b-a}{\lambda}$	19
11	Modal Impedance Z_{12} VS Angular Frequency ω	29
12	Farfield Sound Pressure Amplitude (dB) VS Relative Bearing for $Z_{12} \rightarrow \infty$	31
13	Farfield Sound Pressure Amplitude (dB) VS Relative Bearing for $Z_{12} = 0$	32
14	Normal Mode Amplitudes of Shell VS Mode Number N (Normalized to Fundamental Mode); $Z_{12} \rightarrow \infty$	33
15	Normal Mode Amplitudes of Shell VS Mode Number N (Normalized to Fundamental Mode) $Z_{12} = 0$	34

I. INTRODUCTION

This report is a summary of the developments achieved during the past year in a program of studies to analyze the interactions of sonar domes and transducers during transmission. The program of analysis has been based on an analytical model consisting of a circular cylinder (transducer) and concentric shell (dome). The basic model was developed under previous studies and reported in the summary report for C.Y. 1964.[1]

At the beginning of the past year's study, it was decided that a thorough understanding of the existing model would lead to some elementary guidelines for improved dome design. Accordingly, some improvements were made in the existing model, specifically, an improved description of the velocity distribution on the transducer face; and an evaluation of the dependence of some well-known performance criteria on the parameters of the dome-transducer model was conducted.

As a result of these studies it is now possible to make qualitative statements about the relative importance of the system parameters in determining the effect of the sonar dome on system performance. For example, it is known that the surface density of the dome, i.e., the product of the dome thickness and dome material density, is the most important parameter in determining the acoustic properties of the dome. The stiffness properties (elastic moduli) of the dome material are relatively unimportant in determining acoustic properties. It has been shown that the spacing of the dome relative to the transducer can be a significant factor in determining the radiation impedance at the transducer face and the maximum energy transferred to the medium by the transducer.

These studies have given rough indications for improvements in dome design. However, analytical models of the dome-transducer must be considered as still in the primitive stage.

Analytical and related experimental studies must be pursued in a continuing exploratory development program in order to achieve further improvements in sonar dome design.

II. BACKGROUND

The proper design of a sonar dome must include several aspects including hydrodynamic, strength, durability, and, of course, acoustic properties. While the dome can be studied independently in terms of those requirements, the final design must be a marriage of the results of the various studies and must, therefore, represent a trade-off among each of the requirements. The studies conducted at TRACOR have been directed principally toward the acoustical aspect of dome design. The broad purpose of these studies is to define guidelines for improved sonar performance which can be integrated into a total design concept for domes including hydrodynamic, strength, and durability requirements.

In order to develop an understanding of the acoustical implications of a dome, it is helpful to consider a simple two dimensional cylindrical transducer. The sound pressure p of this transducer can be represented as

$$p = \sum_{n=0}^{\infty} \frac{\delta_n}{H_n^{1\prime}(ka)} H_n^1(kr) \cos n\theta \, e^{-i\omega t} \quad , \qquad (1)$$

where $H_n^1(kr)$ is the first type of Hankel function of argument kr and order n, $k = \frac{\omega}{c}$ with ω the angular frequency, c is the speed of sound in the medium, r and θ are polar coordinates, a is the transducer radius, and the prime indicates a derivative with respect to the argument of the Hankel function. Steady state time dependence of the form $e^{-i\omega t}$ is assumed. The δ_n are Fourier coefficients determined by a specification of the normal particle velocity on the transducer face. Generally, the velocity specification is such that the radiating portion of the transducer is divided into segments having plane wave phasing or time delay and an arbitrary shading, for example, cosine shading.

Equation 1 can be used to compute nearfield and farfield sound pressure distributions, and subsequently determine a two-dimensional directivity index, major lobe width, and side lobe level. The sound pressure at any point in space is determined approximately by a finite number of terms or "modes," the number depending on ka, kr (where r is the point of interest), and the form of δ_n.

If the same cylindrical radiator is surrounded by a concentric elastic shell, the expression describing the pressure, p_2, outside the shell (See Fig. 1.) is[2]

$$p_2 = \sum_{n=0}^{\infty} \frac{\delta_n}{H_n^{1\prime}(ka) + Z_n \alpha_n [J_n'(kb)\, N_n'(ka) - N_n'(kb)\, J_n'(ka)]} \times$$

$$H_n^1(kr) \cos n\theta \, e^{-i\omega t} \quad , \qquad (2)$$

where b is the mean radius of the shell, J_n and N_n are the Bessel and Neumann functions respectively, $\alpha_n = (i\omega\pi b/2\rho c^2) H_n^{1\prime}(kb)$, Z_n is referred to as the modal impedance and the remaining symbols are as previously defined. The shell now can be considered a new radiator which produces the sound field given by Eq. 2. If the sound pressures p and p_2, Eqs. 1 and 2, are compared at some point in space outside the shell (fixed r and θ), they will not, in general, be the same. Hence, the dome affects the sound field produced by the transducer. In order that the dome not affect the transmitted beam it is necessary that Z_n be zero for all values of n ($[J_n'(kb)\, N_n'(ka) - N_n'(kb)\, J_n'(ka)]$ in general is nonzero for a>0, b>0). In general Z_n is nonzero for all except one or two values of n, i.e., one or two terms in Eq. 2. Hence, for the same velocity distribution on the transducer, the pressure field at some distance from the transducer will be different from that of a bare transducer if the transducer is surrounded by a

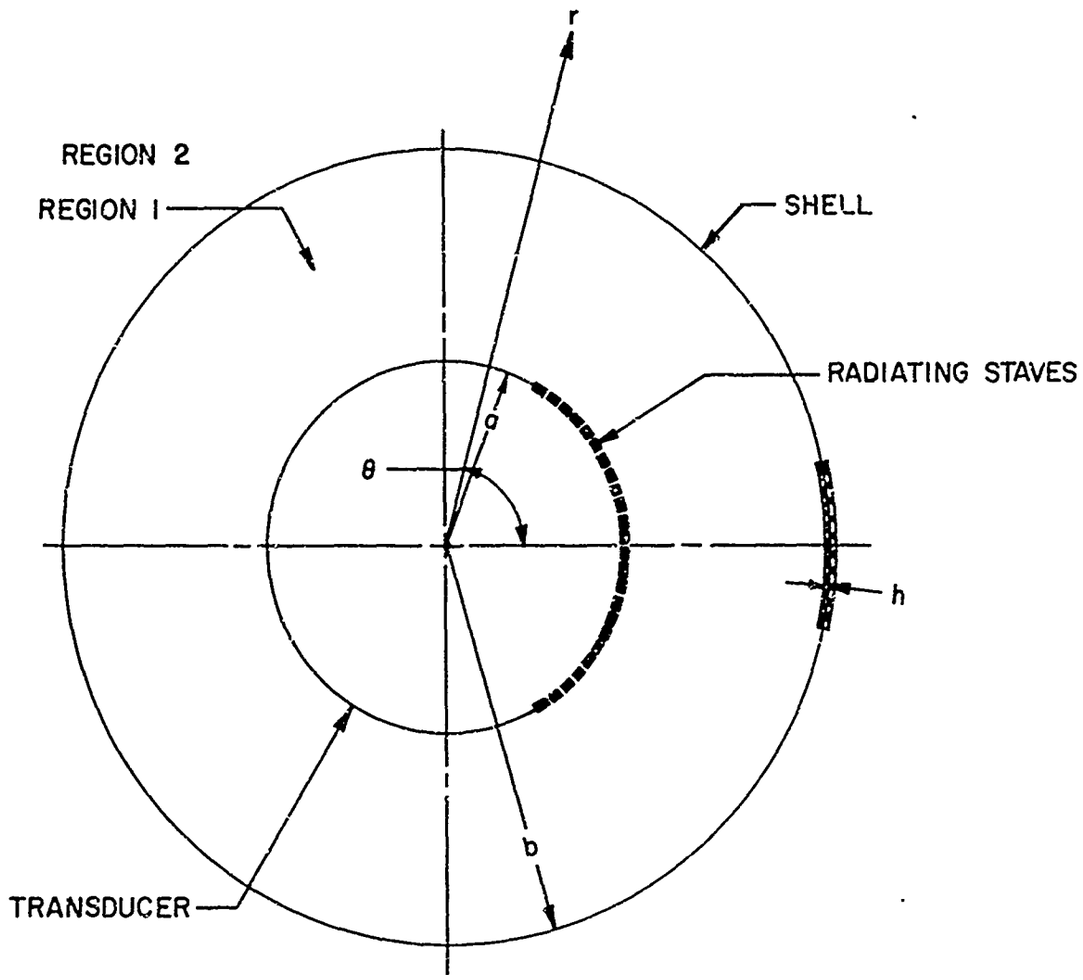

FIG. 1 - GEOMETRY FOR A CYLINDRICAL TRANSDUCER RADIATING IN A CONCENTRIC SHELL

TRACOR, AUSTIN, TEXAS | DWG. 778-1 3/19/65 BM/LBH

concentric shell. Computations of farfield directivity patterns indicate that the presence of the shell results in an increase in the level of the side lobes and a reduction of directivity index compared to a bare transducer.

The shell also affects the sound pressure distribution near the transducer. The general form of the sound pressure p_1 between the shell and transducer is

$$p_1 = \sum_{n=0}^{\infty} [A_n H_n^1(kr) + B_n H_n^2(kr)] \cos n\theta \, e^{-i\omega t} \quad , \qquad (3)$$

where A_n and B_n are constants that depend on δ_n and Z_n, and $H_n^2(kr)$ is the Hankel function of the second kind. The presence of both types of Hankel functions indicates that there are acoustic waves traveling both outward from the transducer and inward toward the transducer. The solution form for a bare transducer, Eq. 1, contains only outward traveling waves. The inward traveling waves represent reflections from the dome which arise due to the impedance discontinuity of the dome. If Z_n were zero for each value of n, then Eq. 3 would reduce to Eq. 1 with $A_n = \frac{\delta_n}{H_n^{1\prime}(ka)}$ and $B_n = 0$. Again, however, Z_n can be zero for only one or two values of n, and the presence of the shell will affect the sound pressure distributions near the transducer compared to a transducer with no shell. Computations of nearfields for transducers with and without shells indicate that the shell significantly alters the radiation loading on the transducer. In addition, the nearfield sound pressure distribution for a transducer with a shell is highly nonuniform compared to the nearfield of a bare transducer.

The present model assumes the dome to be a homogeneous body with no stiffening members. Intuitively one feels that the

addition of stiffening structures to domes will tend to degrade their performance. The effect of stiffening can be visualized by considering that the stiffening members tend to divide the dome up into a series of plates whose edges are constrained. The edge constraints impose a somewhat different vibration response of the dome compared to an unstiffened shell. As a result, it is expected that the stiffening would further distort the farfield pressure distribution. A comparison of some acoustic characteristics of stiffened and unstiffened plates has been carried out elsewhere,[3] and the indication is that the effect of stiffening structure is significant, particularly in terms of increased transmission loss. Unfortunately, the adaptation of analytical methods used in stiffened plate studies to the dome-transducer model is not feasible at this time.

The studies conducted to date have given some insight into the problem of improving the acoustic performance of domes. While the dome impedance cannot be made zero for all modes of vibration, it is possible to reduce the modal impedance for all modes and thereby improve the acoustic properties of the dome (at least for unstiffened domes). The methods for obtaining this improvement are described in the following sections.

III. DISCUSSION OF ANALYTICAL DEVELOPMENTS

This section of the report contains descriptions of the analytical developments in the dome-transducer model during the past year. Some of these developments have been reported in separate technical memoranda,[2,4] and the reader is referred to these for details of the analyses.

A. Improvement of the Transducer Boundary Specifications

As described in Section II, the effects of the sonar dome on transmitted beams have been computed with a mathematical model consisting of a cylinder (transducer) and concentric shell (dome). To form a typical RDT beam, a portion of the transducer elements must be driven in a prescribed manner — usually the elements are phased or time-delayed to straight line and have amplitude shading. In the first analytical model of the dome-transducer, it was not possible to describe the transducer element velocities with discrete amplitudes and phases. It was necessary to describe the velocity amplitude and phase distributions on the transducer face as continuous functions. The first improvement in the dome-transducer model was the development of the procedures necessary to specify discrete values of velocity amplitude and phase for each of the elements used in forming a transmit beam. (The details of this improvement are given in Ref. 4.).

This improvement results in several advantages. First, the model is a more realistic representation of the physical device and one expects the results of the model to predict more accurately the phenomenon being studied. Second, the effect of the dome on transmitted beams for various types of element shading can be predicted. Third, the model can be used to predict the effect of inoperative elements on farfield directivity patterns (by assigning zero velocity amplitude to the inoperative elements) and thereby establish tolerance limits on system performance.

Comparisons of results for the older dome-transducer model and the newer model with improved transducer boundary specification were made in Ref. 4. Significant differences in both farfield and nearfield sound pressure distributions were obtained using the two models. (See Figs. 2 and 3.) The newer model also was used to determine the farfield sound pressure distributions for several types of element shadings. Results for cosine shading and Dolph-Tchebycheff shading are shown in Figs. 4 and 5. These studies indicated that increased side lobe level, the primary effect of the dome on the farfield pattern, was more pronounced for cases of severe shading such as Dolph-Tchebycheff.

B. Parametric Analysis of Dome-Transducer Interactions

More recently, the improved dome-transducer model has been used to compute dome effects for a systematic variation of the model parameters.[2] In particular, the dependence of such performance criteria as directivity index, side lobe level, major lobe width, and transmission coefficient on dome-transducer spacing, dome thickness, density of the dome material, and material properties of the dome was determined. It was found that the most important parameter in determining dome effects is the quantity $\rho_s \omega h$, where ρ_s is the density of the dome material, ω is the angular frequency of the transmitted beam, and h is the thickness of the dome material. The quantity $\rho_s \omega h$ is the dominant term in the expression for the modal impedance of the dome,

$$Z_n = -i\rho_s h\omega + \frac{ih\,E_s}{\omega b^2} + \frac{i\,h^3 E_s}{12\omega b^4}\,[n^4 - 2n^2 + 1] + \frac{i\,h\,n^2 E_s^2}{\omega b^2(\rho_s \omega^2 b^2 - n^2 E_s)}\,, \quad ($$

where Z_n is the ratio of acoustic pressure to normal particle velocity at the mean surface of the dome for the nth term in the sound pressure field expansion. E_s is the elastic modulus

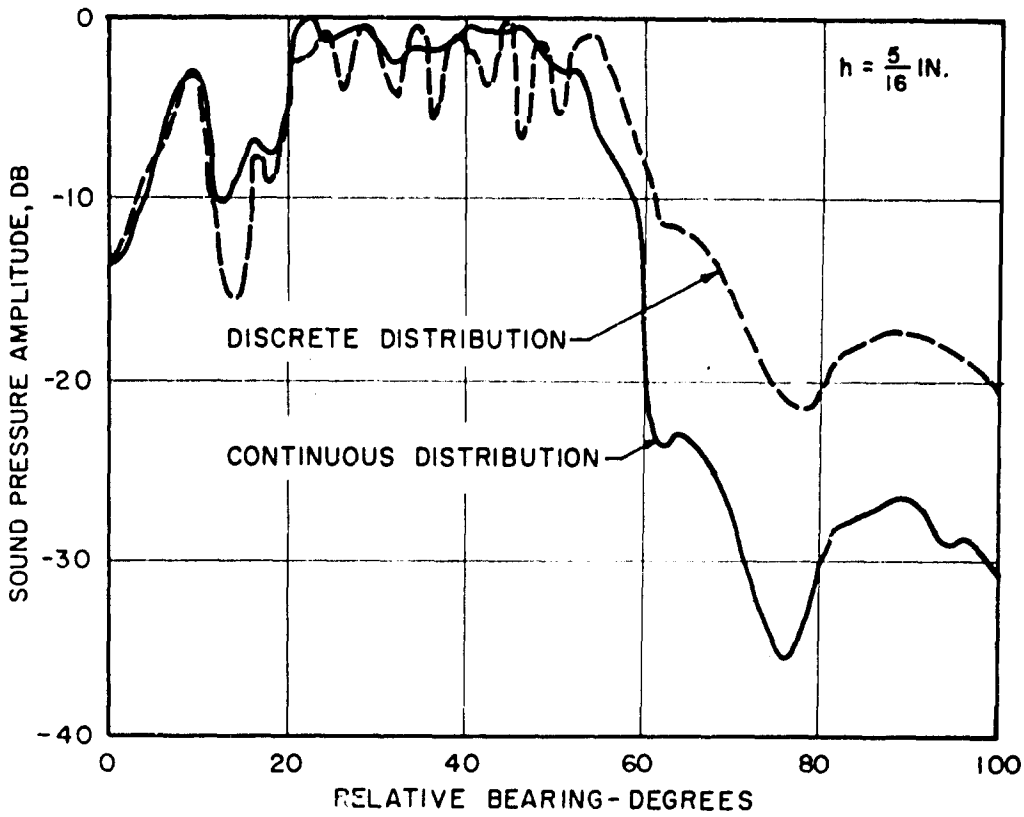

FIG. 2 -SOUND PRESSURE DISTRIBUTION (DB) FOR A TRANSDUCER RADIATING INSIDE A CONCENTRIC DOME (NEARFIELD)

ka = 35.2 kb = 43.9

SHADING = COSINE

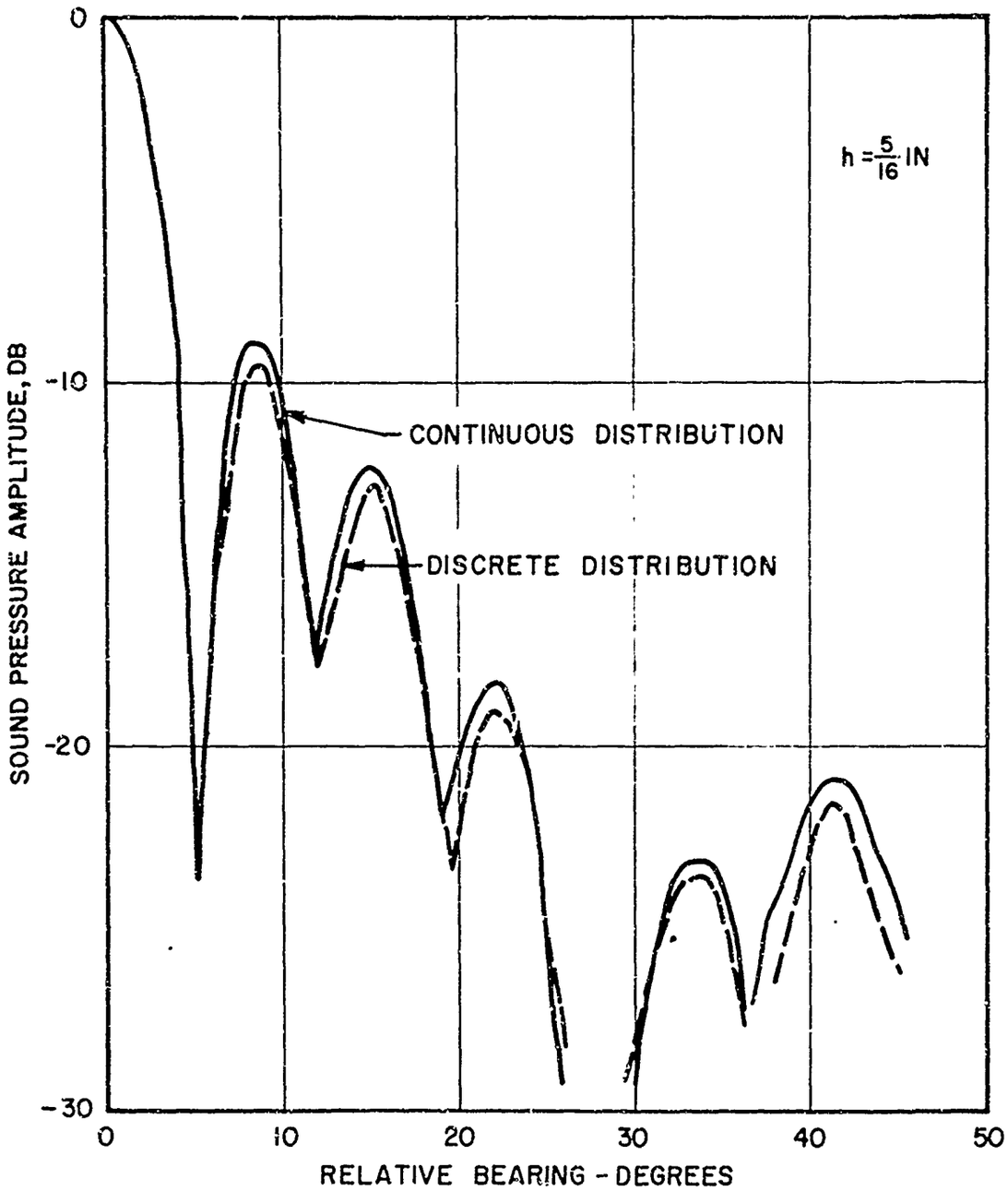

FIG. 3 -SOUND PRESSURE DISTRIBUTION (DB) FOR A TRANSDUCER RADIATING INSIDE A CONCENTRIC DOME (FARFIELD)

ka = 35.2 kb = 43.9

SHADING = COSINE

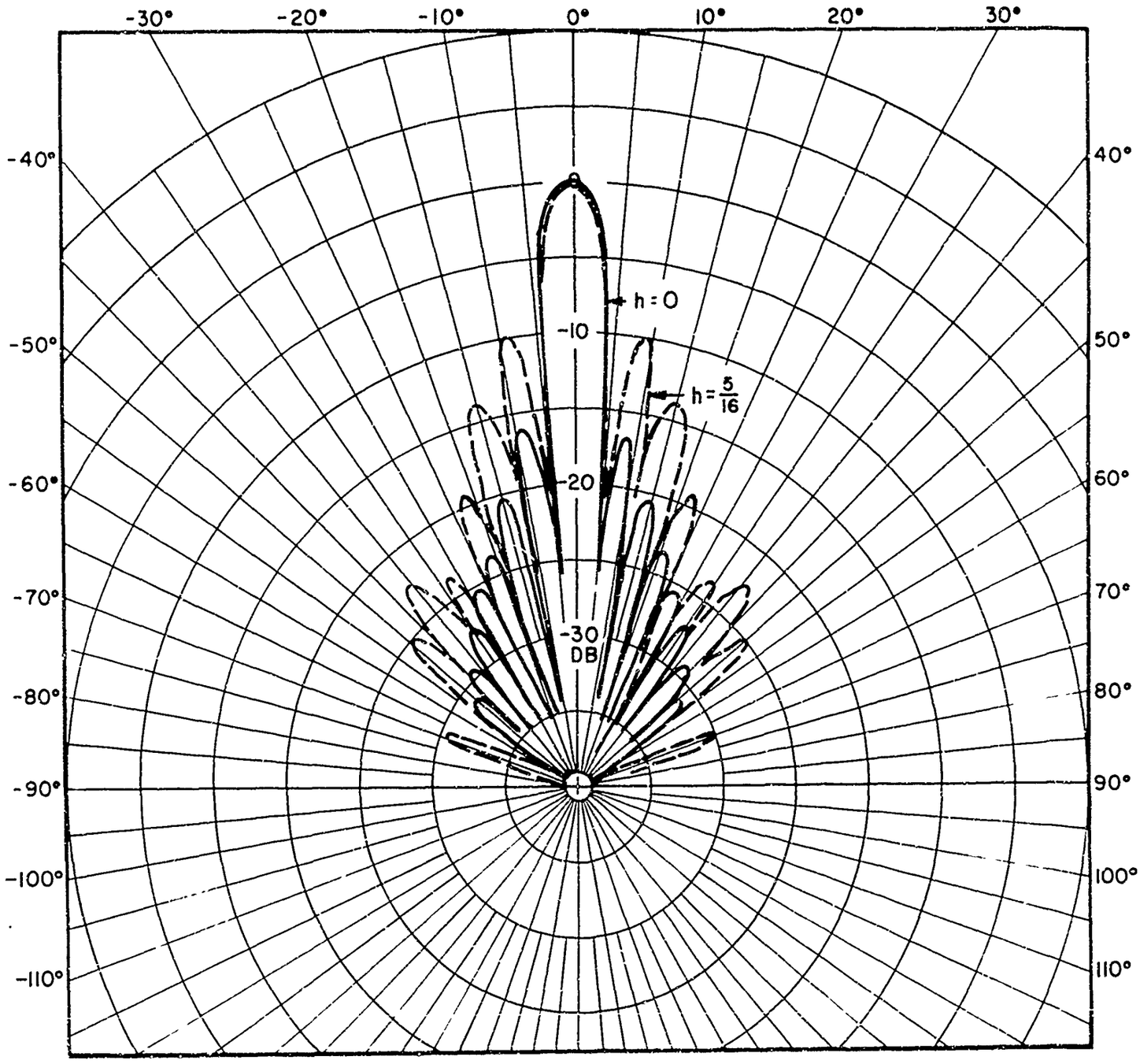

FIG. 4 - COMPARISON OF SOUND PRESSURE DISTRIBUTIONS (DB) FOR A TRANSDUCER RADIATING WITH AND WITHOUT A CONCENTRIC DOME

ka = 35.2 kb = 43.9 r = FARFIELD

SHADING = COSINE

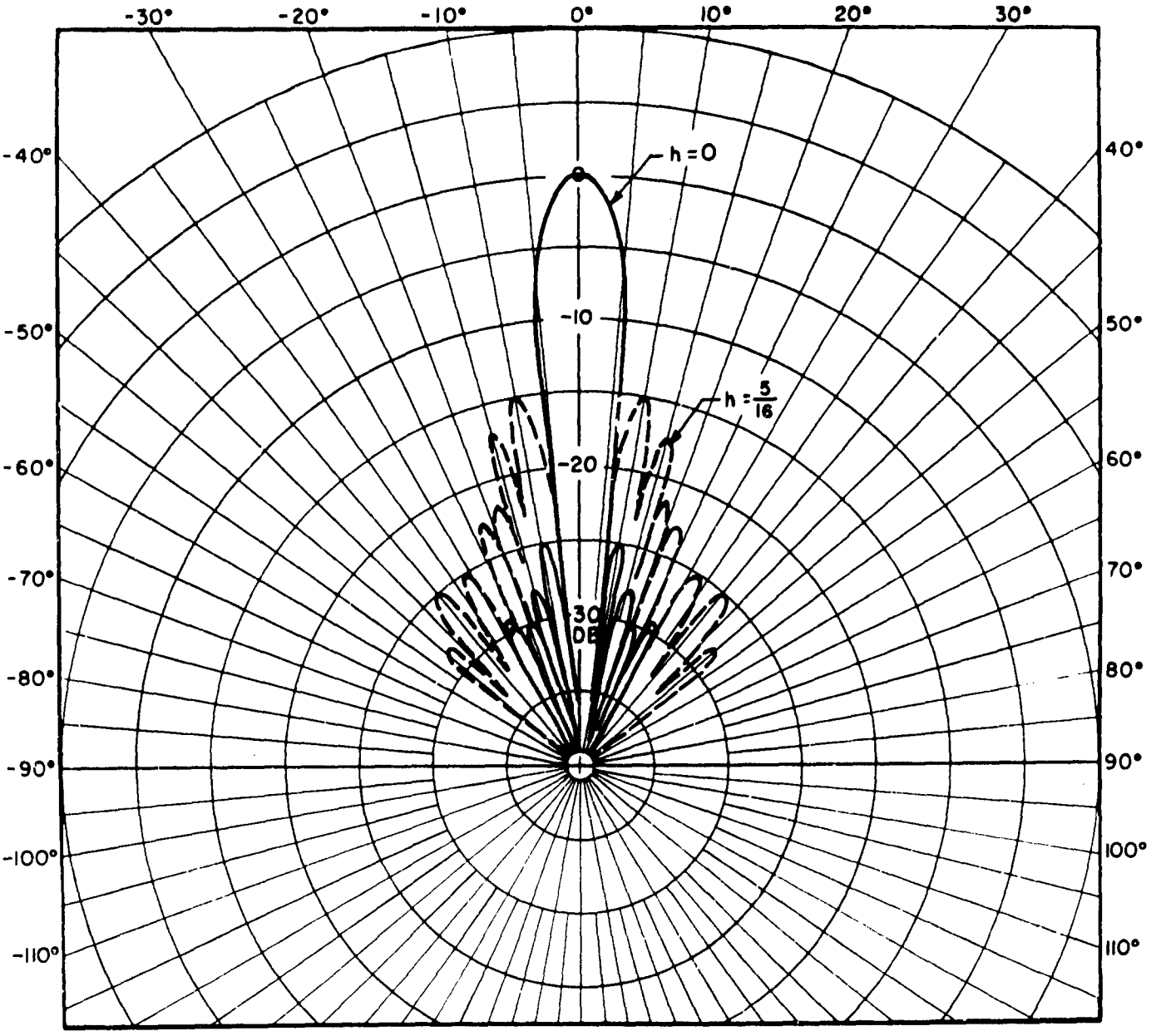

FIG. 5 – COMPARISON OF SOUND PRESSURE DISTRIBUTIONS (DB) FOR A TRANSDUCER RADIATING WITH AND WITHOUT A CONCENTRIC DOME

ka = 35.2 kb = 43.9 r = FARFIELD

SHADING = DOLPH-TCHEBYCHEFF

of the shell material, and b is the radius of the mean surface of the dome.*

Since dome effects are determined principally by $\rho_s h$, for a given transmit frequency ω, it is possible to compact the data given in Ref. 2 to sets of curves which demonstrate the functional dependence of the performance criteria on $\rho_s h$. Some typical curves are shown in Figs. 6-10. Figure 6 indicates the dependence of the two-dimensional directivity index on $\rho_s h$.

Figure 7 shows the variation of side lobe level as a function of $\rho_s h$ and Fig. 8 indicates the dependence of major lobe width on $\rho_s h$. Results for dome transmission coefficient and dome transfer coefficient are shown in Figs. 9 and 10 respectively. The transmission coefficient is a measure of the ratio of power transmitted through the dome to power incident on the dome. Dome transfer coefficient is a measure of the power transferred to the farfield for a transducer with dome as compared to a bare transducer. This latter quantity, a measure of the acoustic coupling of the dome and transducer, is shown as a function of dome-transducer spacing $(b-a)/\lambda$ due to its strong dependence on the spacing parameter. The mathematical definitions of the performance criteria are given in Ref. 2.

C. Viscoelastic Domes

All computed dome effects in the studies to date have assumed that the dome was an elastic body. The application of viscoelastic materials to dome construction, for example the wire-reinforced elastomeric dome for the AN/SOS-26 sonar system, necessitate the investigation of the effects of such materials on dome-transducer interactions.

*It is possible that for a given ω, Z_n may be either quite large or near zero for a fixed n; however, these conditions are relatively unimportant in determining the farfield of the dome-transducer. Resonant dome conditions are discussed in detail in Appendix A.

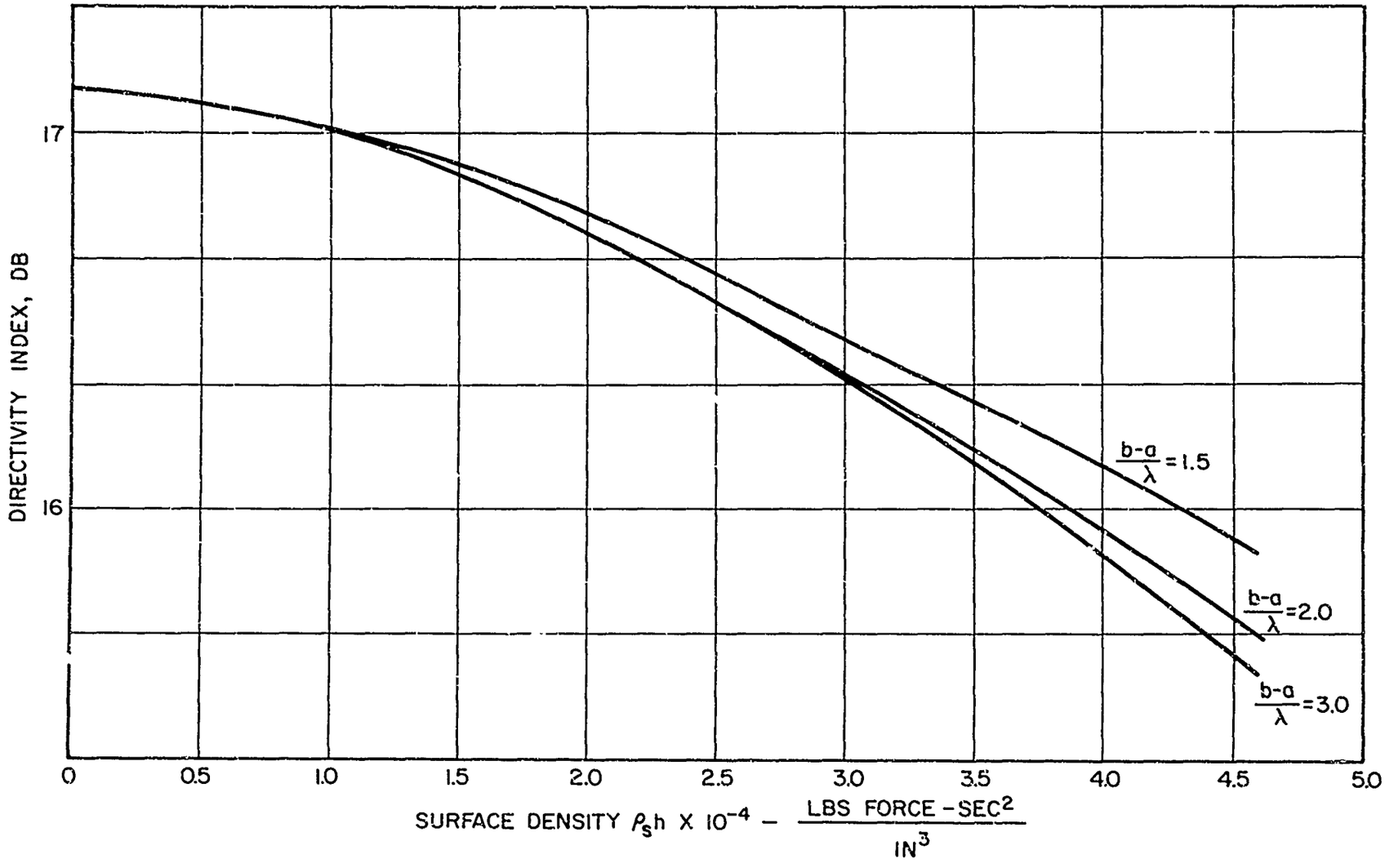

FIG. 6 – DIRECTIVITY INDEX VS DOME SURFACE DENSITY $\rho_s h$

ka = 35.2

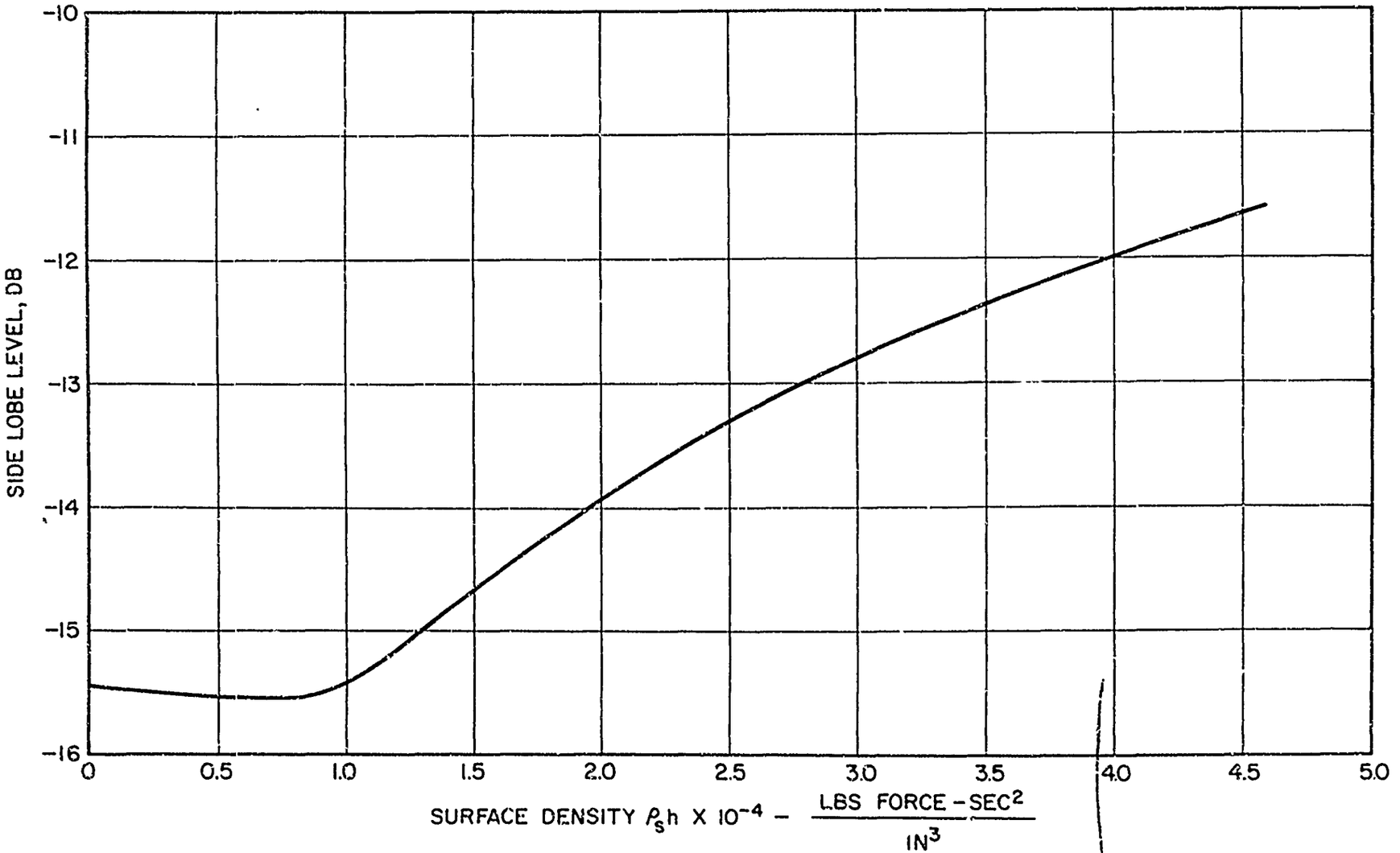

FIG. 7 – SIDE LOBE LEVEL VS DOME SURFACE DENSITY $\rho_s h$

ka = 35.2

TRACOR, INC. AUSTIN, TEXAS 6-2 66 | DWG. 6-12-16 MOYER

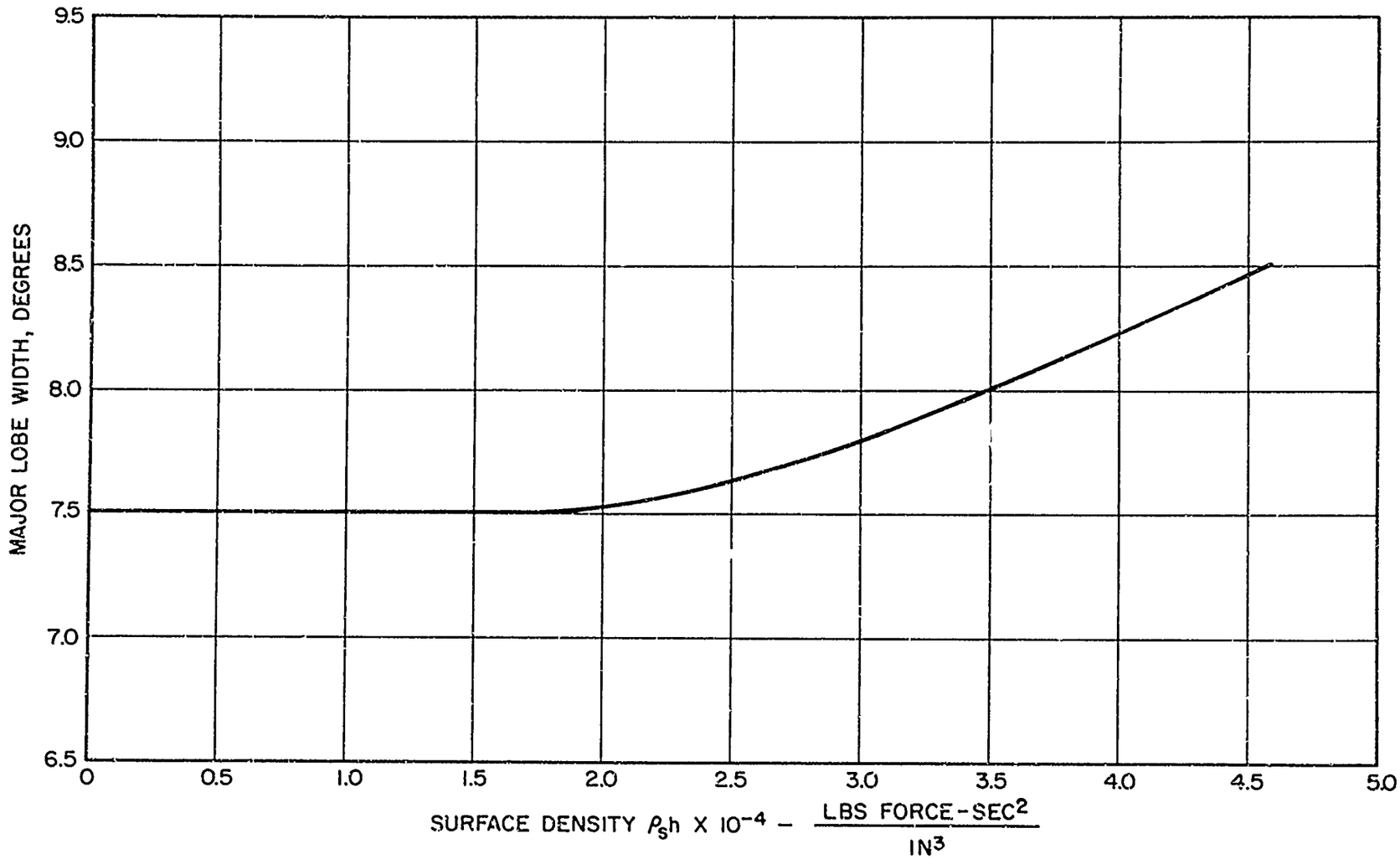

FIG. 8 – MAJOR LOBE WIDTH VS DOME SURFACE DENSITY $\rho_s h$

$ka = 35.2$

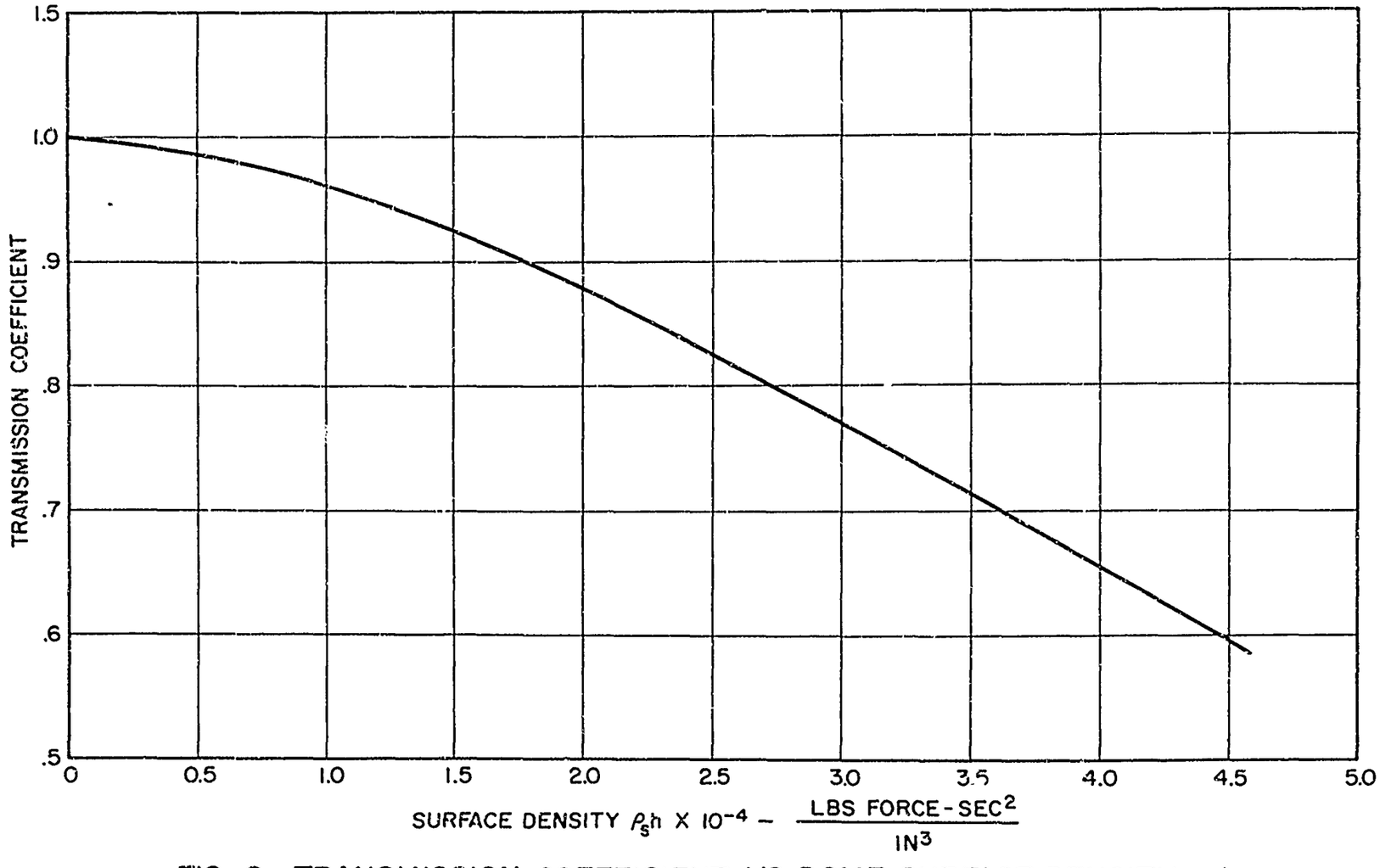

FIG. 9 – TRANSMISSION COEFFICIENT VS DOME SURFACE DENSITY $\rho_s h$

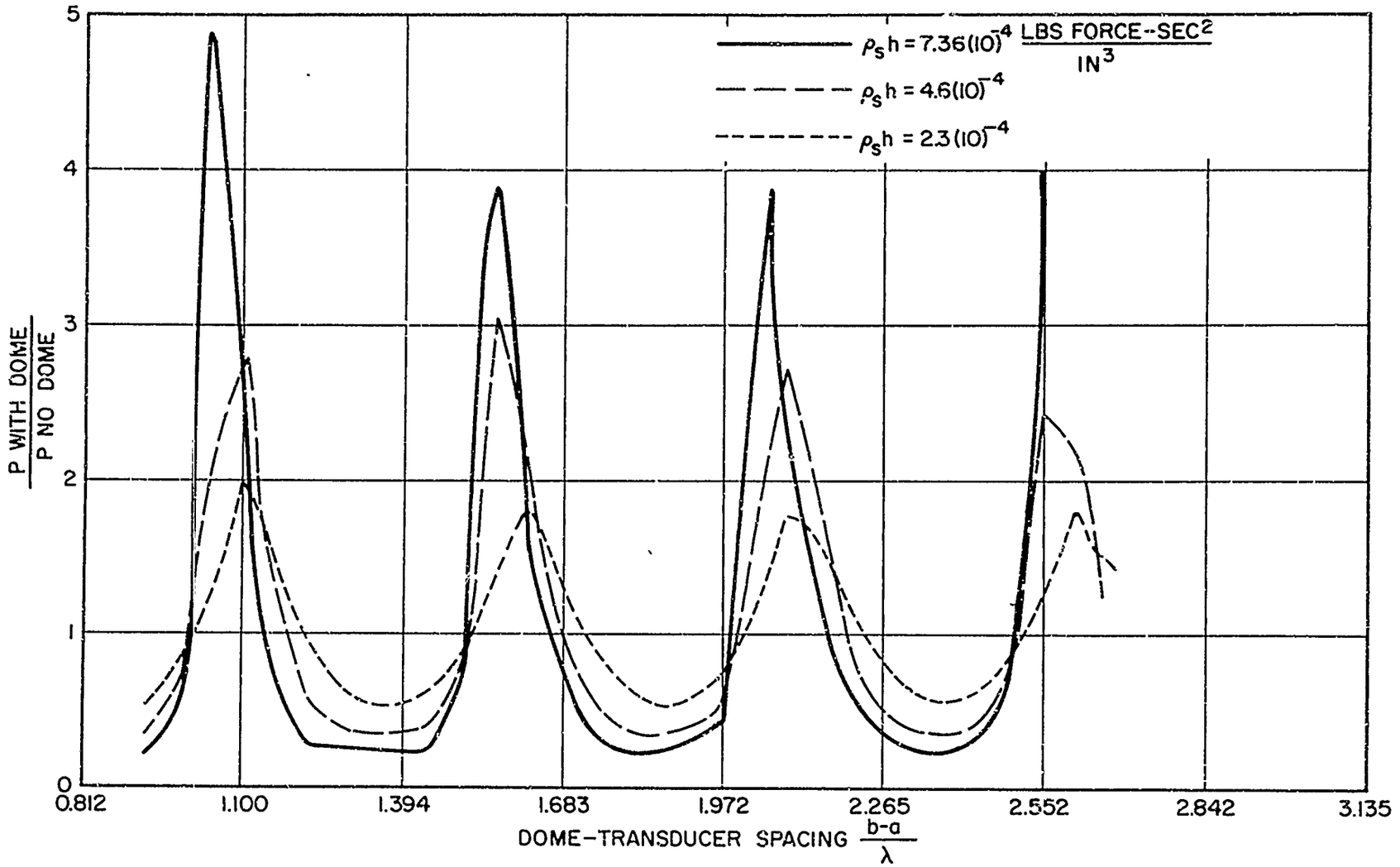

FIG. 10 – TRANSFER COEFFICIENT VS DOME-TRANSDUCER SPACING $\frac{b-a}{\lambda}$

ka = 35.2

It is possible to modify the existing dome-transducer model to include viscoelastic dome materials. This modification requires only a slight change in the form of the differential equations which describe the motion of the dome. As shown in Appendix B, a simple viscoelastic material can be treated in the usual manner if the material constants are complex numbers. (The material constants of elastic materials are real numbers.) The modal impedance of a viscoelastic shell is similar in form to Eq. 4. However, since E_s is complex for the viscoelastic shell, the modal impedance has both real and imaginary parts. Losses in the material are associated with the real part of Z_n. The modal impedance of an elastic material is, of course, purely reactive (imaginary) as shown in Eq. 4.

The only practical problem associated with investigating viscoelastic dome materials is the unavailability of realistic values for the complex moduli. The TRACOR Rockville Laboratory is investigating experimental methods to determine these moduli. No computations of viscoelastic dome effects have been executed to date due to the lack of realistic material constants. However, analysis of the effects of a rubber dome for the AN/SQS-26 sonar system will be conducted for the AN/SQS-26 Project Office, Code 1631, in the near future. The rubber dome and typical steel domes will be compared in terms of the performance criteria previously discussed, using the best estimates available for the viscoelastic moduli.

D. Nonconcentric Dome Shapes

The greatest deficiency of the present dome-transducer model is the unrealistic dome geometry. The next logical improvement in the dome-transducer model is the replacement of the concentric dome with an elliptical one. It is contemplated that the analysis will proceed as in the past, i.e., a solution to the scalar wave equation will be obtained for boundary conditions expressed on the transducer and dome surfaces. Since these

surfaces are expressed in different sets of coordinates, transformations of the solution forms from cylindrical to elliptical coordinates will be required. A basic problem in the development of these transformations is the computation of Mathieu functions which arise in the general solution of the scalar wave equation expressed in elliptical coordinates. Methods for computing these functions generally are not available.

Possible computational methods to be used in the generation of Mathieu functions have been investigated during the past year, and successful methods have been developed to the point that the solution of the boundary value problem appears feasible. Further work on obtaining a solution to the boundary value problem will continue in the studies to be conducted during the following year.

IV. CONCLUSIONS

The studies conducted during the past year lead to the following specific conclusions:

1. The dome causes extreme nonuniformity in the nearfield sound pressure distribution. With no dome, the nearfield sound pressure distribution is relatively smooth. However, the "nearfield roughness" as defined in Ref. 2 increases markedly if the transducer is enclosed in a dome. This effect can increase the radiation loading on transducer elements as well as decrease the cavitation limited source level (through the development of "hotspots" in the nearfield).

2. The presence of a dome increases the side lobe level of the farfield pattern. Shading of the transducer elements to obtain reduced side lobe levels is possible with a dome; however, the side lobe level reduction appears to decrease as the degree of shading increases. Main beamwidth is not affected significantly, but directivity index decreases if the transducer is enclosed in a dome.

3. The energy transmitted to the farfield is attenuated by the dome. The attenuation is due primarily to an interaction between the dome and transducer and not to losses in the dome material. Reflections from the dome change the radiation loading at the transducer face and, consequently, can affect the energy transferred to the surrounding medium. This interaction is dependent on the spacing of the dome and transducer and it may be possible to reduce the interaction by proper spacing of the dome and transducer, at least for limited directions of transmission.

4. Degradations of typical dome-transducer performance criteria such as directivity index depend principally on the surface density (product of mass density and thickness of the dome). As the surface density increases, degradations in the performance criteria increase. The surface density can be shown

to be the dominant factor in the modal impedance of the concentric, unstiffened dome. It is possible that one or two modes of the dome may be in a resonant or antiresonant condition for any given transmit frequency; however, these modes do not control the effects of the dome on transmitted beams.

The above conclusions, again, are based on an elastic, homogeneous dome. Other studies indicate that dome stiffening members can further degrade the acoustic performance of domes.[3]

In addition to studies of the concentric dome model, an extensive investigation of methods for computing Mathieu functions has been completed. These functions are required in order to treat an elliptical dome — a considerable improvement in dome geometry. Successful methods have been derived and the solution of a boundary value problem appears feasible.

Finally, a method of treating viscoelastic materials has been investigated. A simple modification of the differential equations describing shell motions is necessary in order to include viscoelastic effects. The modification entails the replacement of real material constants (elastic body) with complex constants (viscoelastic body). The computation of viscoelastic effects may be a problem due to the scarcity of realistic material constants. The method of computation is simple, however.

V. RECOMMENDATIONS

Continued analytical studies should be directed principally toward improving the dome-transducer model in terms of more realistic geometry. Additionally, methods for treating stiffened shell structures warrant further studies. The desirability of experimental work coordinated with analytical work must be emphasized in an exploratory development program for sonar dome studies.

A three-year program of analytical and experimental studies to improve the understanding of dome-transducer interactions has been submitted to BuShips, Code 1622E.[5] The basic features of this proposal include the following:

1. Studies to improve the geometry of existing dome-transducer models,

2. Extension of studies of dome-transducer interactions to spherical and conformal/planar configurations,

3. Related experimental studies to provide verification of analytical results and assistance in generalizing analytical models.

In particular, studies to be conducted under the first year of the program include the development of a model consisting of an elliptical dome and cylindrical transducer (for which some fundamental research is completed), studies of mathematical tools which have application to the interaction problem independent of system geometry, and experimental measurements of the vibration characteristics of stiffened and unstiffened shells. These experiments will suggest methods of handling stiffened shells mathematically.

These studies are essential to a fundamental understanding of dome-transducer interactions and the subsequent development of improved design guidelines for sonar domes.

VI. REFERENCES

1. An Analysis of the Interaction of the Sonar Dome and Transducer During Transmission (U), TRACOR Document Number 65-188-C, May 17, 1965.

2. A Parametric Analysis of Dome-Transducer Interactions, TRACOR Document Number 66-136-U, February 10, 1966.

3. Sonar Dome Study Analyses, Volume III, Raytheon Report, Ref. Contract NObsr-91145, July, 1965.

4. An Improved Analytical Model of the Interaction of Domes and Transducers During Transmission, TRACOR Document Number 65-292-U, August 31, 1965.

5. Technical Proposal for Long-Range Dome Studies, TRACOR Document Number 65-86-U, August 30, 1965, submitted to BuShips, Code 1622E.

6. M. A. Biot, "Validity of Thin Plate Theory in Dynamic Viscoelasticity," J. Acoust. Soc. Am., Volume 35, p. 796.

7. W. Flügge, Stresses in Shells, Springer-Verlag, Berlin, 1962, p. 219.

VII. ACKNOWLEDGEMENTS

The program of studies described in this report was conducted under the leadership of W. C. Moyer. He was assisted by R. E. Douglass, Karolen Glass, K. B. Hamilton, J. D. Morell, and E. A. Tucker.

APPENDIX A

The sound pressure field outside the concentric dome is given by the expression

$$p_2 = \sum_{n=0}^{\infty} \frac{\delta_n}{H_n^{1\prime}(ka) + Z_n \alpha_n [J_n'(kb)\, N_n'(ka) - N_n'(kb) J_n'(ka)]} \times$$

$$H_n^1(kr) \cos n\theta \, e^{-i\omega t} \qquad (2)$$

where the symbols are defined in Sec. II. As discussed in Sec. II, if Z_n, the modal impedance of the dome, were zero for all values of n, the dome would not affect transmitted beams. However, Z_n is not equal to zero except possibly for one mode (one value of n). It is also possible that $Z_n \to \infty$ for one value of n, in which case the amplitude of that particular mode (term) becomes zero. These two distinct features of Z_n and the resulting effects on transmitted beams are discussed in this appendix.

The modal impedance, Z_n, of the shell is given by

$$Z_n = -i\omega\rho_s h + \frac{iE_s h}{\omega b^2} + \frac{iE_s h^3}{12 b^4 \omega}(n^4 - 2n^2 + 1) + \frac{iE_s^2 n^2 h}{\omega b^2 (b^2 \omega^2 \rho_s - E_s n^2)} \qquad (4)$$

where ω is the angular frequency, ρ_s is the mass density of the shell, h the thickness of the shell, $E_s = \frac{E}{1-\nu^2}$, E is Young's modulus, ν is Poisson's ratio, and b is the mean radius of the shell.

The behavior of the impedance equation exhibits two distinct features. At the angular frequency given by

$$\omega_\infty = n\left(\frac{E_s}{\rho_s b^2}\right)^{\frac{1}{2}} , \qquad (5)$$

$Z_n \to \infty$, an antiresonance condition. This condition results since the denominator of the last term of Eq. 4 reduces to zero. At angular frequencies given by

$$\omega_o = \left(\frac{E_s}{2\rho_s b^2}\right)^{\frac{1}{2}} \left\{\left[1 + \frac{h^2}{12b^2}(n^4 - 2n^2 + 1) + n^2 \pm \sqrt{\left[1+\frac{h^2}{12b^2}(n^4 - 2n^2 + 1) + n^2\right]^2 - \frac{h^2}{3b^2}(n^6 - 2n^4 + n^2)}\right]\right\}^{\frac{1}{2}}, \quad (6)$$

$Z_n = 0$, a resonance condition. Equation 6 is obtained by setting Z_n in Eq. 4 equal to zero and solving for ω_o. The solution of Eq. 6 has two real roots, hence there are two frequencies for which $Z_n = 0$.

The angular frequency associated with $Z_n \to \infty$ differs for each mode, (value of n) but has a unique number, $\left(\frac{E_s}{\rho_s b^2}\right)^{\frac{1}{2}}$, associ- with each choice of the parameters. There are two angular frequencies associated with $Z_n \to 0$ for each choice of the above parameters. For a fixed value of n, the angular frequency for which $Z_n \to \infty$, lies between the two angular frequencies for which $Z_n = 0$. As the modal number increases, both zero-impedance angular frequencies increase, but they are never equal nor is either one equal to the angular frequency for which Z_n is undefined. The behavior of Z_{12}, a typical modal impedance, is shown as a function of ω in Fig. 11.

The question arises as to what distortion of the transmitted beam would occur if the operating frequency $f = 2\pi\omega$ were chosen close to $\omega_o/2\pi$ or $\omega_\infty/2\pi$ for some particular mode of the dome? In order to examine this situation ω_o and ω_∞ were determined for n = 12 and typical values of the parameters ρ_s, h, and E_s.

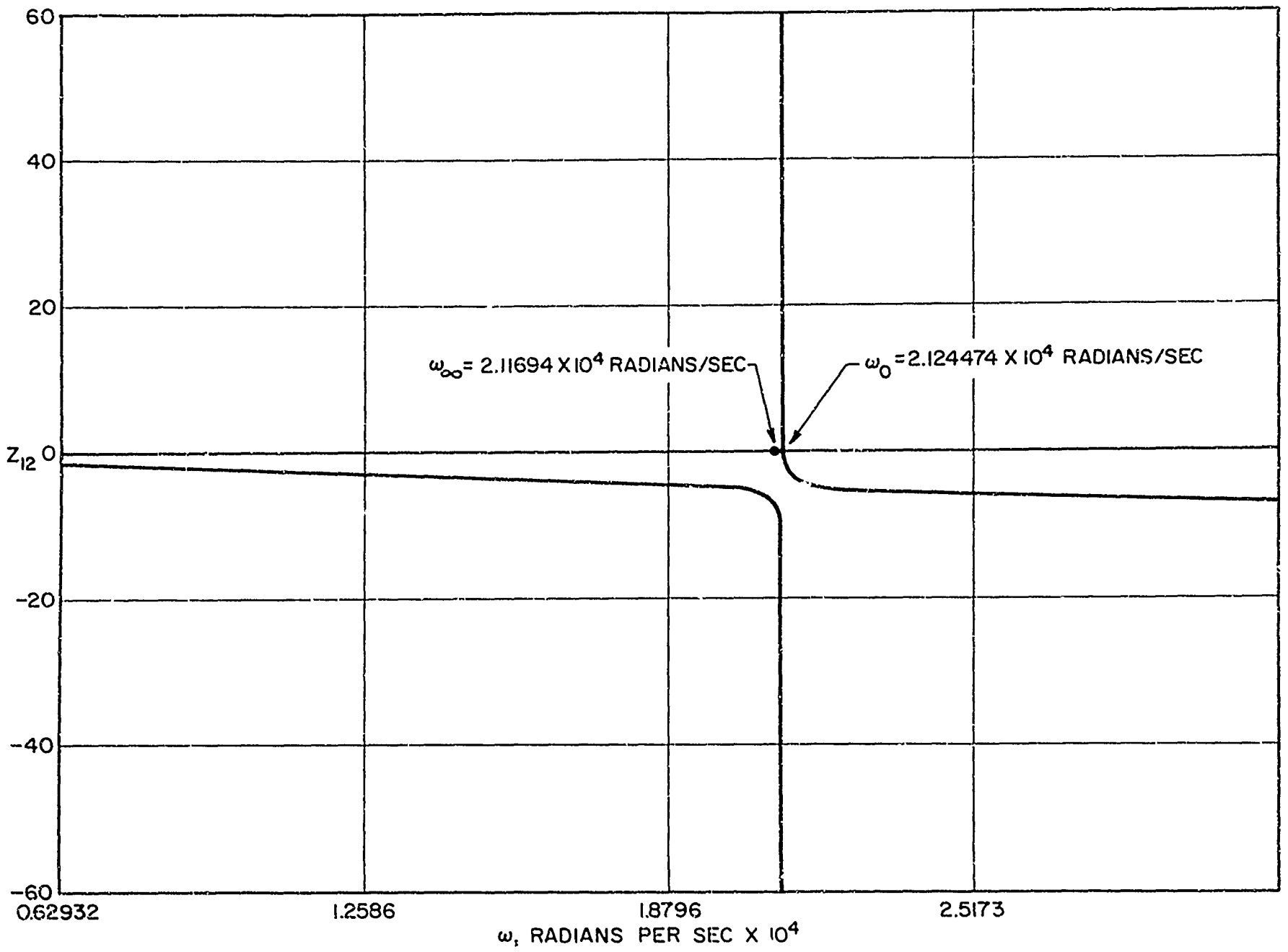

FIG. 11 - MODAL IMPEDANCE Z_{12} VS ANGULAR FREQUENCY ω

$E = 3 \times 10^7 \frac{LB}{IN^2}$ $\quad \nu = 0.3$ $\quad \rho_s = 7.355 \times 10^{-4} \frac{LB\text{-}SEC^2}{IN^4}$ $\quad h = 0.3125$ IN

TRACOR, INC. | DWG. 6-12-22
AUSTIN, TEXAS 6-2-66 MOYER

The value of $\omega_\infty \big|_{n=12} = 2.11694(10)^4$ rad/sec for which $Z_{12} \to \infty$ was obtained from Eq. 5. Two values of ω_o were obtained from Eq. 6. These were $\omega_o \big|_{n=12} = 2.124474(10)^4$ rad/sec and $1.89007(10)^2$ rad/sec, for which $Z_{12} = 0$. Computations of farfield patterns using the values $\omega = 2.11694(10)^4$ rad/sec and $\omega = 2.124474(10)^4$ rad/sec were carried out and the results are shown in Figs. 12 and 13. As shown in the figures no essential difference in the patterns is observed. (Any differences likely are due to the difference in ka of the transducer rather than modal resonance or antiresonance effects.)

In addition to the farfield patterns, modal amplitudes were obtained for $0 \le n \le 100$ for the two frequencies ω_o and ω_∞. These are shown in Figs. 14 and 15. In Fig. 14 it is seen that the modal amplitude for n = 12 is zero as expected, since $Z_{12} \to \infty$. For $Z_{12} = 0$ (Fig. 15), the modal amplitude reduces to $\frac{\delta_{12}}{H_{12}^{1\prime}(ka)}$ as discussed in Sec. II.

From these results it can be concluded that driving the shell at a resonant or antiresonant frequency for any one mode does not distort the beam unduly, i.e., more than would be expected at a nearby frequency. This result is due to the fact that only one or two modes can be in a resonant or antiresonant condition for any given angular frequency ω. (It may happen that ω_∞ for a low order mode may be nearly equal to the lower value of ω_o for a higher order mode.); and this mode, bounded in magnitude between zero and $\frac{\delta_n}{H_n^{1\prime}(ka)}$, does not control the total response of the dome.

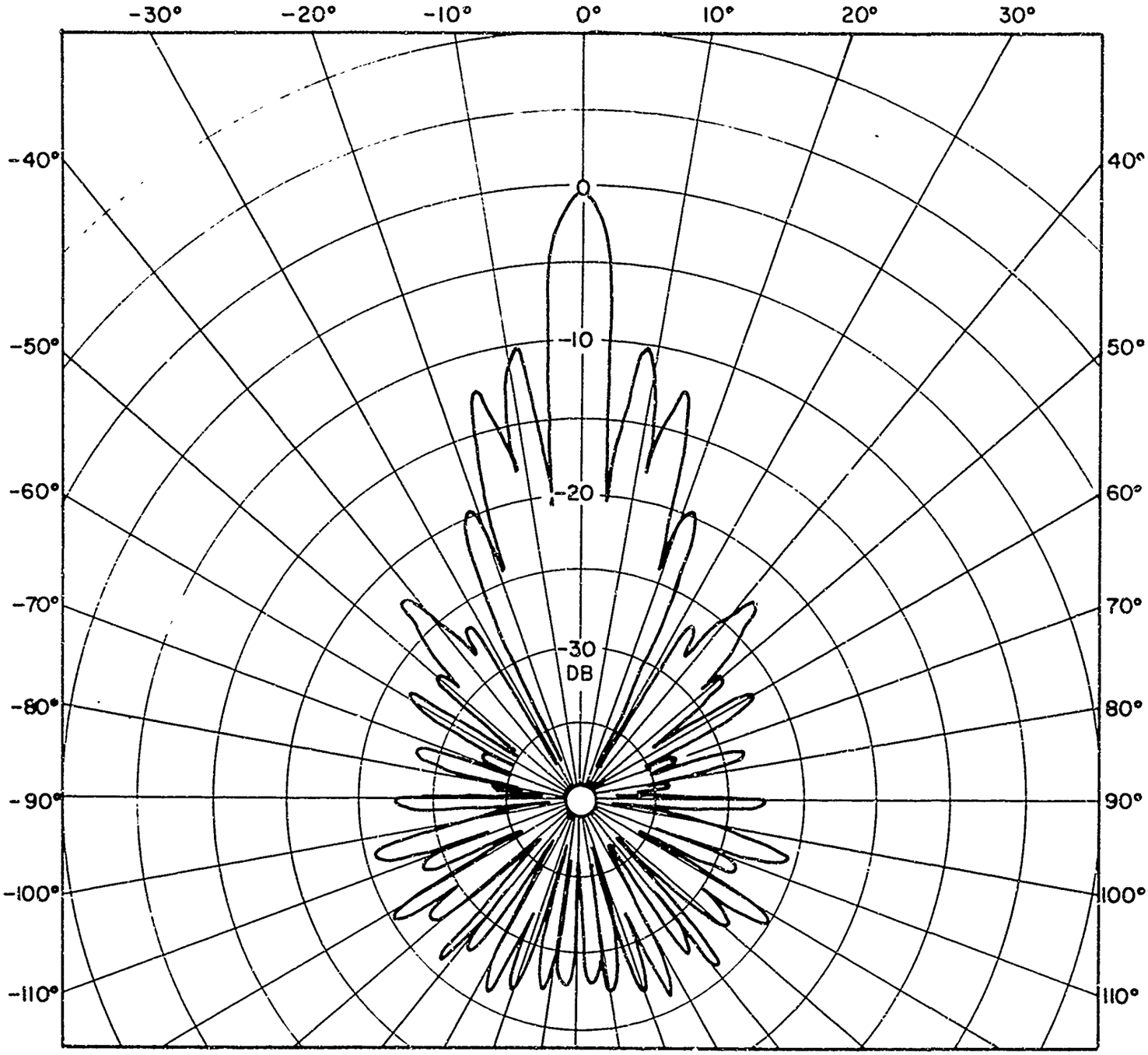

FIG. 12-FARFIELD SOUND PRESSURE AMPLITUDE (DB) VS. RELATIVE BEARING FOR $Z_{12} \rightarrow \infty$ ($\omega = 2.11694 \times 10^4$ RADIANS/SEC)

$\upsilon = 0.3$ $E = 3 \times 10^7$ PSI $\rho_s = 7.355 \times 10^{-4} \frac{\text{LBS FORCE-SEC}^2}{\text{IN}^4}$

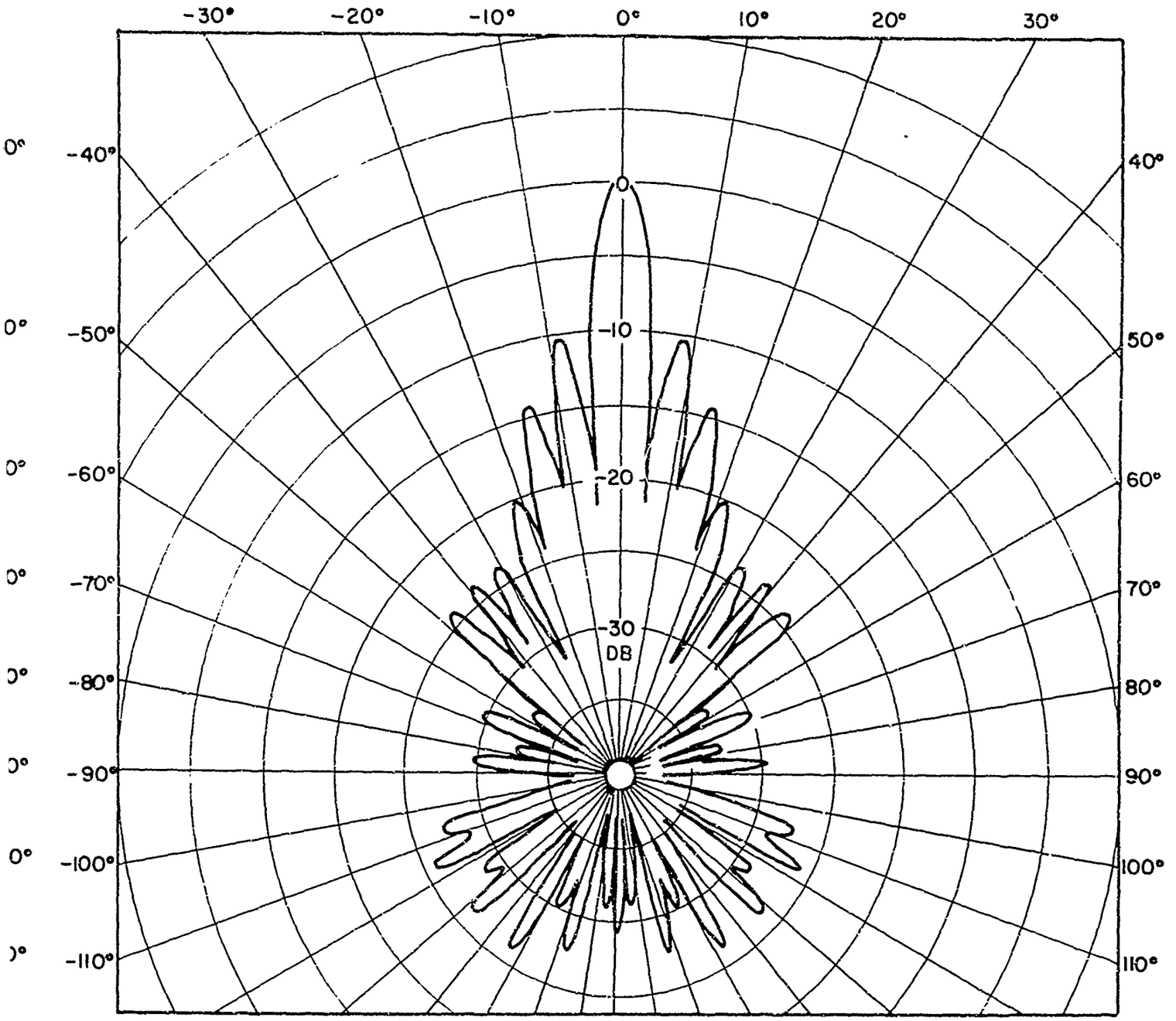

FIG. 13-FARFIELD SOUND PRESSURE AMPLITUDE (DB) VS RELATIVE BEARING FOR $Z_{12} = 0 (\omega = 2.124474 \times 10^4$ RADIANS/SEC)

$\nu = 0.3$ $E = 3 \times 10^7$ PSI $\rho_s = 7.355 \times 10^{-4} \frac{\text{LBS FORCE-SEC}^2}{\text{IN}^4}$

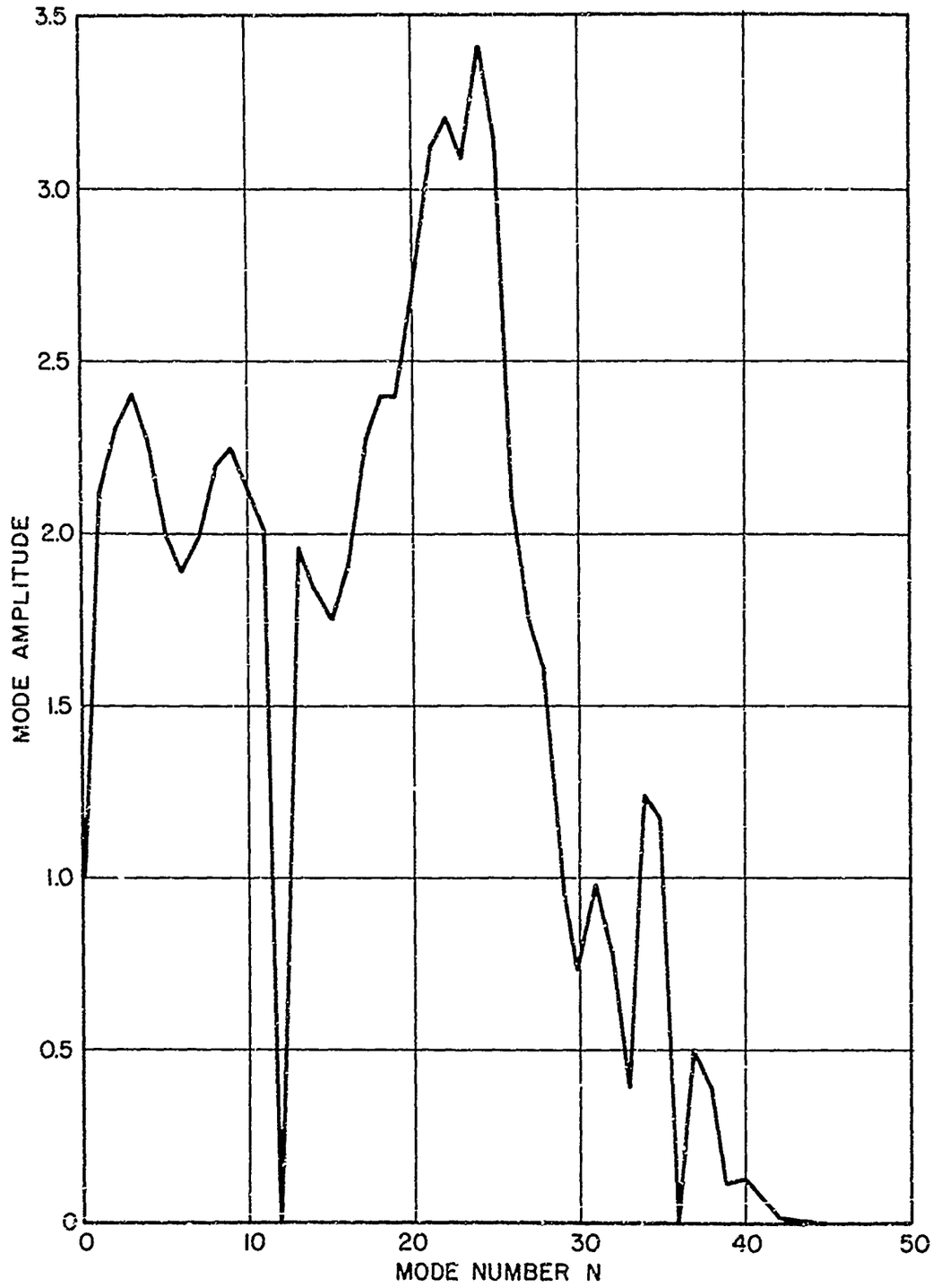

FIG. 14- NORMAL MODE AMPLITUDES OF SHELL VS MODE NUMBER N (NORMALIZED TO FUNDAMENTAL MODE) $Z_{12} \longrightarrow \infty$

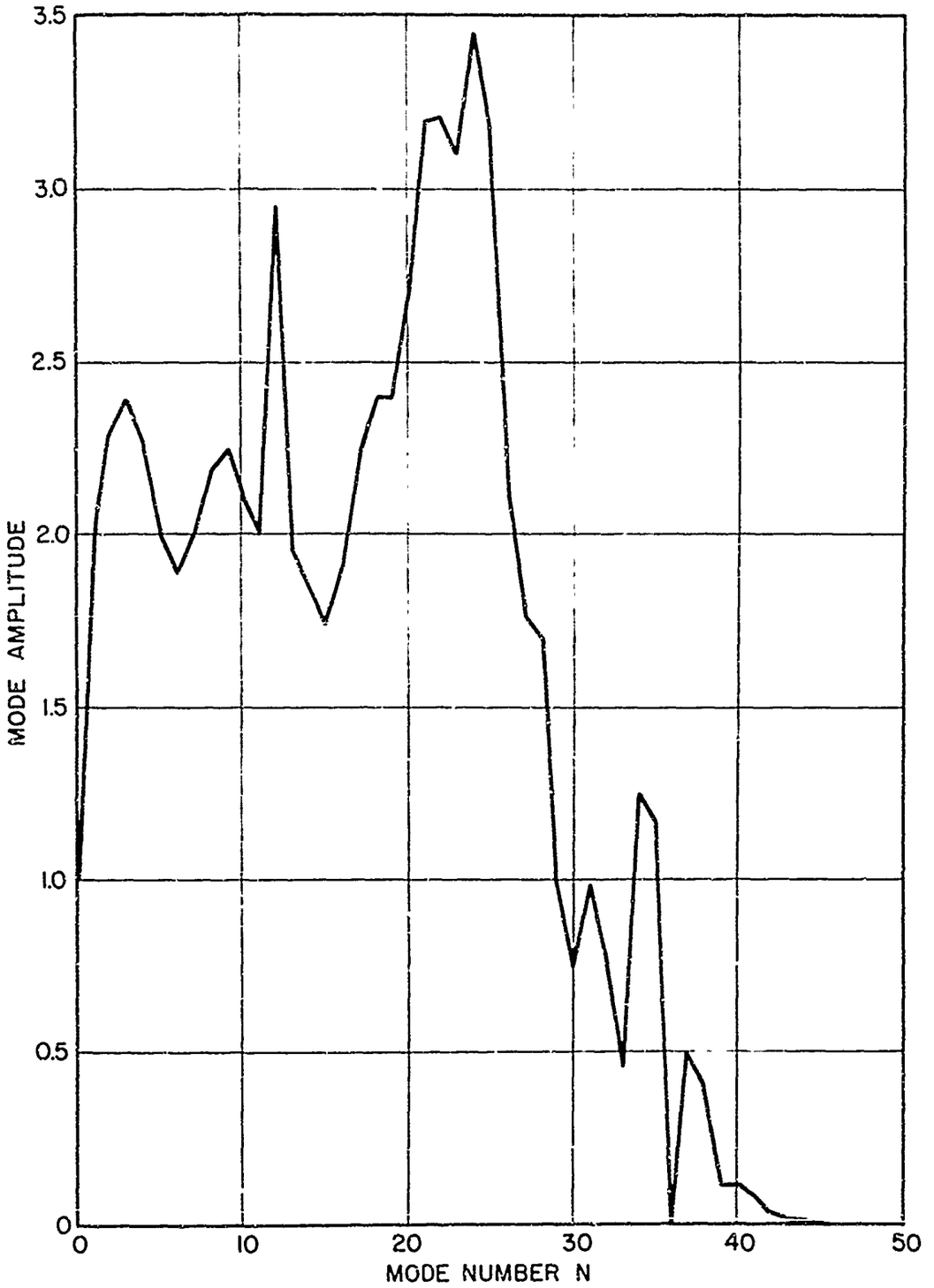

FIG. 15 – NORMAL MODE AMPLITUDES OF SHELL VS MODE NUMBER N (NORMALIZED TO FUNDAMENTAL MODE) $Z_{12} = 0$

APPENDIX B

This appendix presents a method of accounting for energy dissipation within a viscoelastic dome material. The equations of motion for the shell model of the dome are based on a stress strain relation of the form,

$$\sigma = E_s \, \epsilon \quad , \tag{7}$$

where ϵ is the longitudinal strain, σ is the longitudinal stress, and E_s is a stiffness parameter. For the case of homogeneous, isotropic, elastic shells, E_s is called the plate modulus and can be written in terms of the Young's modulus E and the Poisson ratio ν of the shell material, $E_s = E/(1-\nu^2)$.

Energy losses in sound transmission through a medium are explained in terms of a viscous dissipation mechanism. This phenomenon is included by adding one term to the stress strain relation,

$$\sigma = E_s \, \epsilon + \mu \frac{d\epsilon}{dt} \quad , \tag{8}$$

where μ is the viscosity coefficient and t is time. This dependence of the stress on the strain and the strain rate describes the simplest type of viscoelasticity. For steady state vibration with angular frequency ω, the stresses and strains can be considered to have an $e^{-i\omega t}(i = \sqrt{-1})$ time dependence. Then Eq. 8 takes the form

$$\sigma = [E_s - i\omega\mu]\epsilon \quad . \tag{9}$$

Equation 7 and Eq. 9 have the same form. The correspondence of Eq. 7 and Eq. 9 suggests that the shell equations for a viscoelastic shell may be obtained from those for an elastic shell by simply making E_s complex. The validity of using a complex elastic modulus in thin plate theory is discussed in Ref. 6.

The Flügge equations for a cylindrical shell are differential equations for the shell displacements as functions of the angle θ, which varies from $-\pi$ to π on the shell surface.

Let the radial and tangential displacements from equilibrium of the middle surface of the shell be denoted by u_r and u_θ, respectively. Flügge's shell equations are[7]

$$\rho_s \frac{\partial^2 u_\theta}{\partial t^2} = \frac{E_s}{b^2}\left[\frac{\partial^2 u_\theta}{\partial \theta^2} + \frac{\partial u_r}{\partial \theta}\right] \tag{10}$$

$$\rho_s \frac{\partial^2 u_r}{\partial t^2} = \frac{p_- - p_+}{h} - \frac{E_s}{b^2}\left[\frac{\partial u_\theta}{\partial \theta} + u_r\right] - \frac{E_s h^2}{12 b^4}\left[\frac{\partial^4 u_r}{\partial \theta^4} + 2\frac{\partial^2 u_r}{\partial \theta^2} + u_r\right] . \tag{11}$$

where h is the thickness of the shell and b is the radius of its middle surface, ρ_s is the mass density of the shell material and p_- and p_+ are the pressures on the inside and outside shell surfaces, respectively.

These equations determine the motion of a viscoelastic shell with the complex value of E_s defined by Eq. 9. The determination of the sound pressure field produced by a transducer radiating inside a concentric viscoelastic shell is then obtained in a manner exactly analogous to that for an elastic shell.

END

DATE

FILMED

7-8-66